Water crystallisation in highly concentrated carbohydrate-based systems

Lopez-Quiroga, Estefania; Fryer, Peter; Bakalis, Serafim; Wang, Rui; Gouseti, Ourania

DOI:
10.1021/acs.cgd.8b01648

Document Version
Peer reviewed version

Citation for published version (Harvard):
Lopez-Quiroga, E, Fryer, P, Bakalis, S, Wang, R & Gouseti, O 2019, 'Water crystallisation in highly concentrated carbohydrate-based systems', *Crystal Growth and Design*, vol. 19, no. 4, pp. 2081-2088. https://doi.org/10.1021/acs.cgd.8b01648

Water crystallisation in highly concentrated carbohydrate-based systems

Rui Wang[a], Ourania Gouseti[b], Estefania Lopez-Quiroga[a], Peter J. Fryer[a], Serafim Bakalis[ab]*

[a]School of Chemical Engineering, University of Birmingham, B15 2TT, UK

[b]Faculty of Engineering, University of Nottingham, Nottingham, NG7 2RD, UK

*e.lopez-quiroga@bham.ac.uk

ABSTRACT Water crystallisation was studied at a range of concentrations (20%-60% solids) in sucrose and gum arabic systems. Increasing sucrose concentration reduced nucleation temperature by 26 °C compared to equilibrium values; crystal growth rates decreased by up 95% (from $8x10^{-5}$ m/s with 40% sucrose to $4x10^{-6}$ m/s with 60% w/w) for 7 °C supercooling, while addition of carboxymethyl cellulose (CMC) - higher viscosity - resulted in 40% slower growth rates (60% sucrose). Ice crystal shape changed from dendritic (-16 °C) to rounded edges (-24 °C) as temperature decreased. For gum arabic, increasing supercooling (from 2 °C to 10 °C) resulted in faster growth rates (up to 3 times) for the 50% system, while the 60% solution showed rates < $6x10^{-6}$ m/s. Controlling water crystallisation during freezing is critical in manufacturing of frozen/freeze-dried (bio)products, although little information is available on the behaviour of concentrated systems (i.e. >40% solids). Despite presenting significant challenges (i.e. limited water availability and mobility), processing such concentrated systems could increase energy

efficiency, as less water is processed. Results from this systematic investigation of crystal growth kinetics in concentrated carbohydrate systems demonstrate that crystal growth can be promoted despite kinetic limitations and reveal potential to reduce energy demand during freezing/freeze-drying by processing less water.

KEYWORDS water crystallisation; crystal growth; carbohydrates; high solid concentration

1 Introduction

Freezing is an important processing and preservation operation in food manufacturing that involves lowering the temperature of the material below its freezing point [1,2]. During freezing part of the water crystallises to ice, and the acquired ice morphology largely determines the quality and properties of the frozen foods. For example, during freezing of fish, meat and vegetables, large number of small sized ice crystals are usually preferable to small number of large sized crystals, as large crystals may penetrate the cell walls causing tissue damage and consequent loss of quality[3,4]. Ice cream is another representative example, where ice crystal size determines mouthfeel: too large and the ice cream feels 'gritty'; too small and the ice cream melts too easily[5,6]. Freezing is also the first step of freeze-drying, in which the frozen ice crystals are further sublimated, leaving a dry, porous structure[7,8]. Again, it is important to effectively control ice crystal formation, as the porosity and properties of the dried food largely depend on the ice crystal morphology created during the first freezing step[6].

Ice crystal morphology depends on the formulation and freezing conditions, which affect nucleation and growth. Nucleation is stochastic[9] and, although some mechanisms – e.g. addition of ice crystal seeds in secondary nucleation - can increase the repeatability of crystallisation[10], it is difficult to control. Similarly, crystal growth will be determined by a series of factors (e.g. formulation, process conditions) that can complicate ice crystal formation.

The inherent complexity of crystallisation is increased when freezing low-water content systems due to the reduced water availability for crystal formation and the increased system's viscosity that limits molecular mobility[10,11]. In addition, water crystallisation temperature will decrease in concentrated systems, moving closer to the glass transition temperature, where water mobility is again very limited[12]. Kinetic and operational limitations combine to result in a narrow working area, as illustrated in Figure 1 for the water-sucrose system[14].

Such limitations might be overcome by adding ice crystal seeds to promote water crystallisation[13]. After adding the seed, water molecules diffuse to and are incorporated into the crystal lattice structure forming a stable nucleus that can grow to a larger crystal. Seeded systems are used in applications such as freeze concentration of fruit juice[14] or water waste treatment[15], but have not been exploited for structuring purposes. In addition, secondary nucleation can occur at much lower supercooling – i.e. higher temperatures - than primary nucleation[9,16]. This can be advantageous in terms of energy demand: operating at higher temperatures implies lower refrigeration loads and thus economic and environmental benefits. Research that helps to understand and control crystallisation phenomena in high concentrated systems is thus needed.

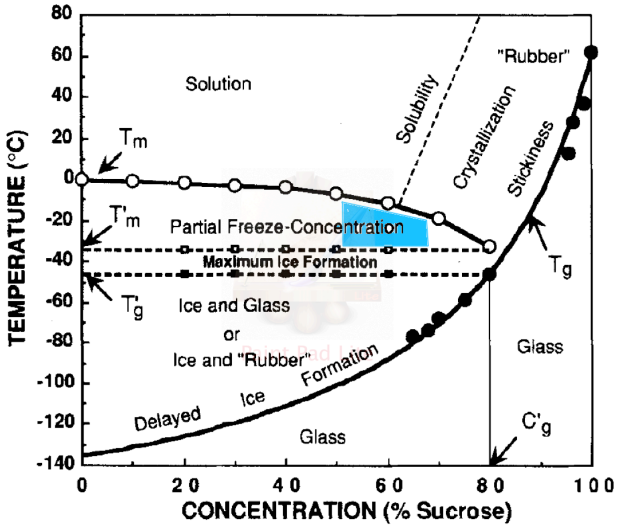

Figure 1. Adapted phase diagram of the water-sucrose system [14]. The blue area represents the potential working area for industrial applications of high concentrated systems freezing processes.

The aim of this work is to give better understanding of water crystallisation mechanisms at a range of solute concentrations, with a focus on carbohydrate-based systems. Primary crystallisation was investigated by Differential Scanning Calorimetry (DSC) and cryo-X-ray diffraction in sucrose systems up to 60% solids. Likewise, an optical method has been developed that allows visualisation of crystallisation under a microscope and it was used to study crystal growth in concentrated systems. To illustrate the methodology, the effect of temperature, concentration, viscosity and formulation on crystal growth kinetics and morphology was investigated.

2. Materials and methods

2.1 Materials

Sucrose solutions (20%, 30%, 40%, 50%, and 60% solids w/w) were prepared by mixing the solute with distilled water while stirring (Stuart CB162 hotplate stirrer) at room temperature until the solution was clear. Gum Arabic solutions were prepared by adding powder to distilled water under vigorous stirring until reaching final concentrations of 50% and 60% solids w/w. The beaker was then covered and stirring was maintained until the solute was fully dissolved (typically 24 h-36 h). Foam formed during gum arabic systems preparation was manually discarded. Sucrose/CMC (carboxymethyl cellulose) solutions were prepared with a fixed water content (40% w/w): one with 59% sucrose and 1% CMC, and the other with 59.5% sucrose and 0.5% CMC. In those, sucrose was first dissolved, and the required CMC amount was then added and mixed at room temperature until full dissolution was achieved.

2.2 Methods

2.2.1 Differential Scanning Calorimetry (DSC)

The thermal behaviour of the sucrose solutions (20%-60% w/w) was investigated on a Mettler Toledo DSC2 differential scanning calorimeter. Around 20 mg (exact weight recorded) of each solution was placed into a 40 μL aluminium pan that was then sealed and the material was cooled down from room temperature to -70 °C and reheated to 20 °C at constant rate of 1 °C/min. All scans were triplicated using a sealed empty pan as reference. The fraction of ice formed during crystallisation (primary nucleation) can be calculated from DSC results using [17,18]:

$$Ice\ fraction = \frac{\Delta H}{\Delta H_w} \qquad (1)$$

where ΔH (J g^{-1} sample) is the area below the DSC peak for each sample divided by the sample's exact weight and $\Delta H_w = 334$ J g^{-1} is the latent heat of fusion of water.

2.2.2 Cryo-X-Ray Diffraction (Cryo-XRD)

Cryo-X-Ray diffraction curves for the 60% sucrose solution were obtained in a powder diffractometer (Siemens D5000) equipped with an Oxford low temperature cryostream. Of the investigated sucrose systems, this is the one with the highest concentration and thus the most challenging in terms of crystallisation – and therefore the most interesting and relevant one. Approximately 0.01 mL of the solution was cooled down from room temperature to -70 °C and then reheated to 20 °C at a constant rate of 1 °C/min to replicate the DSC experimental conditions. Experiments were conducted in triplicate, with the samples being scanned at: -20 °C, -30 °C, -40 °C, and -70 °C.

2.2.3 Optical experiments

Ice crystal growth has been further monitored by adding an ice seed into the supercooled concentrated solution. The apparatus used for the experiments combines a temperature-controlled stage (Linkam, LTS 120) with an optical microscope (Leica Z16 APO). The peltier stage ensures temperature stability and accuracy (±0.1 °C), while a camera mounted on the microscope allows crystal growth to be recorded.

During these experiments, one droplet (0.1 mL) of the concentrated sample was emptied into the cavity of a single-cavity glass slide and it was placed onto the peltier stage. A smaller droplet (10% sucrose solution for experiments with sucrose and distilled water for experiments with gum arabic) was also placed onto the cooling stage to create the seeds. The system was then cooled down at 1 °C/min, to the desired supercooling. Once the temperature reached this value (accuracy and

stability ensure by the peltier stage control), the seed was added into the centre of the supercooled droplet, and subsequent growth was recorded (1 frame per second).

2.2.4 Crystal growth measurements

Image analysis of the crystallisation snapshots was carried out (ImageJ software) to measure experimental crystal growth rates. A typical post-processing image is shown in Figure 2(a), where the white area in the centre is the crystallised region and the dark area that surrounds the crystal is the supercooled liquid (the bright circle is the reflection of the microscope's lighting, which was ignored during image processing).

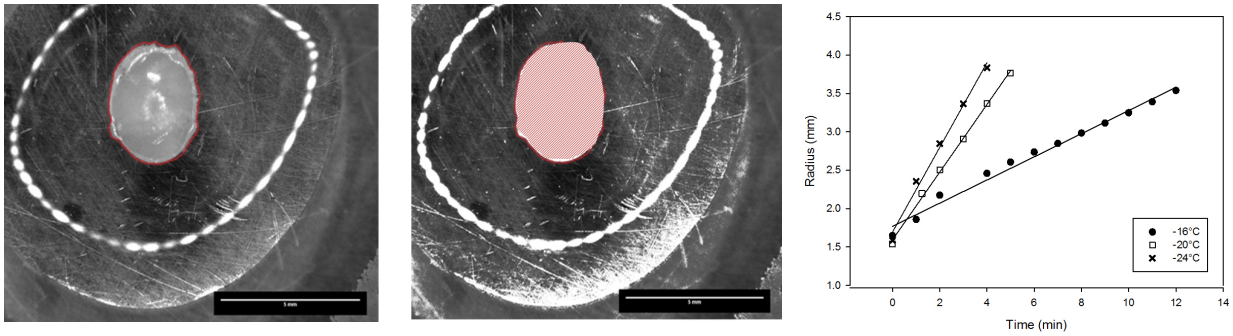

(a) (b) (c)

Figure 2. Example of image processing (scale bar 5 mm). (a) Image of ice region with its edge enclosed; (b) Same crystallised region with its area highlighted. This area was assumed to be a disk, and an equivalent radius was calculated from it; (c) Radius of the equivalent area calculated using Equation (1). The slope of the straight lines (best fitting to a first order polynomial) defines the growth rate of the system.

The area S (mm^2) of the solid region was measured (see Figure 2(b)) and the radius r (mm) of an area-equivalent circle calculated using:

$$r = \sqrt{\frac{S}{\pi}} \tag{2}$$

The equivalent radii r were plotted as a function of time (see Figure 2(c)), and the growth rate was determined as the slope of the best linear fitting.

Three different seed volumes were tested (1 μL, 3 μL, and 5 μL) to evaluate the effect of the seed size on the crystal growth rate, and showed little effect on ice crystal growth kinetics (data not shown). Therefore, for the optical experiments a volume of 3 μL was used to create the seed as this was large enough to handle easily and small enough to allow space for crystal growth observations under the microscope.

2.2.5 Activation Energy

The activation energy of the process is related to the crystal growth rate via an Arrhenius-type relationship[14,19,20]:

$$G = Ae^{\left(\frac{-E_a}{RT}\right)} \tag{3}$$

where G is the growth velocity (m/s), E_a is activation energy (J mol^{-1}), R is gas constant (J mol^{-1} K^{-1}), T is the absolute temperature (K) and A (m s^{-1}) is a pre-exponential factor. The apparent activation energy E_a can be estimated from the slope of an Arrhenius plot[21], where ln$G$ is plotted against the inverse of the absolute temperature $1/T$. Similarly, the activation energy required for diffusion-controlled growth, E_a^D (J mol^{-1}), can be estimated from a plot of lnD_{sw} vs. 1/T [21], where D_{sw} (m s^{-1}) is the self-diffusivity of water in the supercooled solution, which can be calculated through[22]:

$$ln\frac{D_{sw}}{D_{w,0}} = -\frac{\Delta E}{RT} - \frac{y_w \hat{V}_w^* + \zeta y_s \hat{V}_s^*}{y_w(K_{ww}/\gamma)\left(K_{sw} - T_{g,w} + T\right) + y_s(K_{ws}/\gamma)\left(K_{ss} - T_{g,s} + T\right)} \quad (4)$$

where ΔE is the activation energy, $D_{w,0}$ is a constant and y_w and y_s are the mass fractions of water and solute, respectively. The Free-Volume parameters (K_{ww}, K_{sw}, K_{ws}, K_{ss}, $\hat{V}_w^*$, $\hat{V}_{ws}^*$, ζ γ) are all available in literature[22] for relevant carbohydrate systems. If $E_a > E_a^D$, then the growth process is either temperature or kinetic-controlled[21].

3 Results and discussion

3.1 DSC (Enthalpy measurements)

DSC freezing curves for the sucrose solutions (20% - 60% concentration) are shown in Figure 3(a). All samples exhibited an exothermal peak during cooling corresponding to water crystallisation (primary nucleation). Increasing sucrose concentration decreased the onset temperature of crystallisation from -19 °C (for the 20% solution) to -37 °C (for the 60% solution). These crystallisation temperatures are lower than reported[14] equilibrium freezing temperatures obtained from a DSC melting curve. At equilibrium, the freezing and melting temperatures coincide and for the 60% sucrose systems the authors reported equilibrium freezing temperature of -11.4 °C. The difference between the crystallisation temperature determined during freezing and the equilibrium freezing temperatures (up to 26 °C difference for the 60% solids system) reflects the increasing supercooling required for crystallisation (primary nucleation) to occur.

Figure 3(b) shows the crystallisation enthalpy ΔH (J g^{-1} sample) as a function of solids concentration, together with the data expected if all the water in the sample was solidified ΔH_{ideal} (J g^{-1} sample):

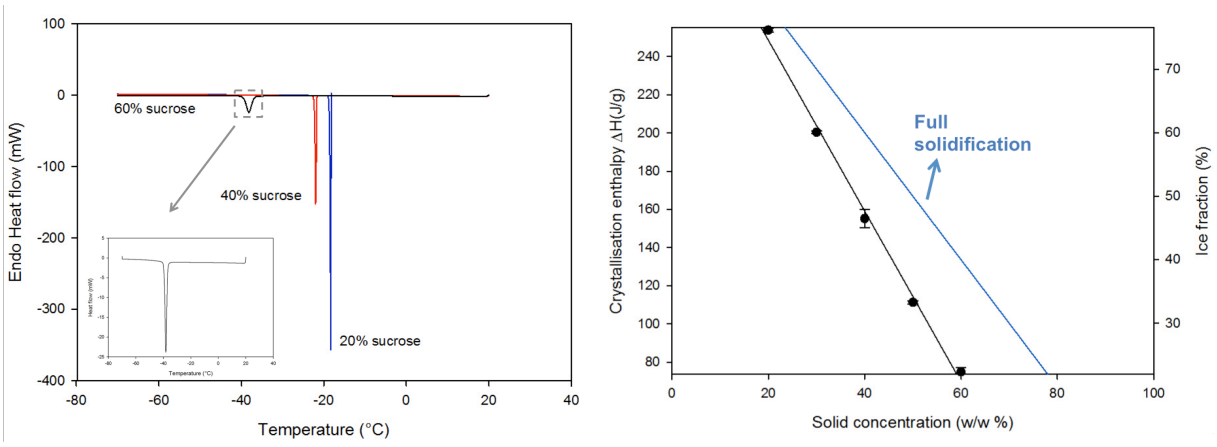

(a) (b)

Figure 3. (a) Differential Scanning Calorimetry (DSC) thermograms of sucrose solutions (20%, 40%, 60% solids) with a cooling rate of 1 °C/min. The magnified figure shows the crystallisation peak of the 60% system. (b) Absolute value of enthalpy change of water crystallisation at different sucrose concentration (dots: experimental data; line: linear fitting). Experiments were triplicated and error bars are not distinct as they are smaller than the size of the dots.

$$\Delta H_{ideal} = (1 - solid \cdot fraction)\Delta H_w \quad (5)$$

The measured ΔH values decreased monotonically on increasing sugar concentration from approx. 255 (J g^{-1} solution) for the 20% sucrose solution to 74 (J g^{-1} solution) for the 60% sucrose system. This dependence of ΔH on the solids content of the system can be fit to a linear model[23,24]:

$$\Delta H = A - Bw_s \quad (6)$$

where w_s (wt. %) is the solids concentration and the estimated constants are A=338 J g^{-1}, and B=4.5 J g^{-1}.

As crystallisation progresses, freeze-concentration occurs in the non-crystallised portion of the system. The maximum ice content (strongly dependent on cooling rates) was estimated by linear extrapolation from Equation (6) to $\Delta H=0$ J g^{-1} [19,24,25], resulting in a maximum concentration of *ca*. 76% for sucrose. This agrees with reported values ranging between 69% and 78% [23-25]. Ice fraction values obtained using Equation (1) are presented in Figure 3(b), showing a reduction on ice formed from 76% to 22% as the solids increased from 20% to 60%.

3.2 X-ray Diffraction

Primary crystallisation was further studied using low temperature X-ray diffraction and results for the 60% sucrose solution are summarised in Figure 4(a). Samples were first cooled from room temperature to -70 °C and then heated to room temperature at a constant rate of 1 °C/min. Scans were conducted at -20 °C (i), -30 °C (ii), -40 °C (iii) and -70 °C (iv) during cooling, and then -40 °C (v), -30 °C (vi) and -20 °C (vii) during heating. In order to reduce potential annealing effects due to the scanning process (each scan requires approximately 10 min acquisition time at the selected temperature), different scans in Figure 4(a) were acquired in separate cooling/heating cycles. Direct comparison of the peak intensities between scans is therefore limited.

No crystal peaks can be seen in data sets (i) and (ii), indicating that neither water nor sucrose crystallisation occurred on cooling the solution at temperatures higher than -30 °C. This may be attributed to the high viscosity of the 60% solids solution and the sparse spatial distribution of water[26]. On further temperature reduction (≤-40 °C and up to -70 °C) peaks at 22.7°, 24.1°, 25.6°, 39.9°, 43.6° and 47.2° are evident - see data set (iii) and (iv) in Figure 4(a) - and can be identified as ice crystals peaks[27]. Water crystallisation took place at a temperature between -30 °C and -40 °C, which in agreement with the DSC cooling curve of the same (60% sucrose) system that showed

an exothermal peak at -37 °C (Figure 3(a)). No sucrose crystals were observed within the temperature range studied, which is in accordance with the sucrose-water phase diagram shown in Figure 1 [19].

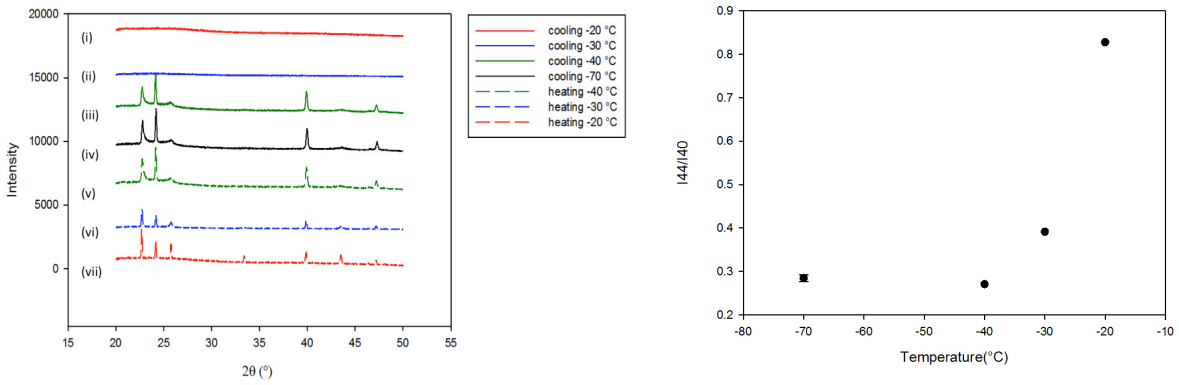

(a) (b)

Figure 4. (a) X-ray diffraction patterns for the 60% sucrose solution. (b) Intensity ratio I44/I40 calculated from XRD patterns (iv, v, vi and vii) as a function of temperature during heating of 60% sucrose.

During heating from -70 °C to -20 °C, the crystal structure persisted even at -20 °C (see graph (vii) in Figure 4(a)). However, as the temperature increased, the peak intensities in the XRD scans changed. For example, there was a shift in the highest peak from that at 24.1° in the -40 °C scan to that at 22.7° in the -20 °C scan (see data sets (v) and (vii) in Figure 4(a)). This change in the crystal peak patterns indicates a transition of ice crystals into different forms as discussed below.

Three different main forms of frozen water can be identified at atmospheric pressure: hexagonal crystal, cubic crystal, and amorphous[26]. In XRD scanning, hexagonal ice crystals are indicated by

peaks at 22°, 24°, 26°, 34°, 40°, 44° and 47°, while cubic ice crystals show peaks at 24°, 40°, and 47° coincidently[26]. Cubic ice is a metastable form and it is typically the form acquired during freezing of water to temperatures above -80 °C [28]. Below this temperature, ice is usually in hexagonal form[29]. Cubic ice will typically transform to hexagonal with time and the rate of transformation strongly depends on temperature[28]. The ratio of hexagonal/cubic ice can be calculated from the intensity ratio of the peaks at 44° and 40°: I_{44}/I_{40} [30]. The minimum value is 0, when all the ice is in cubic form. This will gradually increase as the percentage of hexagonal ice increases in the system until a maximum value at 0.8, which indicates that all the ice is in hexagonal form - the value of 0.8 is the intensity ratio of peak 44° and 40° for pure hexagonal ice[26,27]. Intensity ratios calculated from Figure 4(a) are displayed in Figure 4(b). For temperatures ≤-40 °C, the scans indicated a mixture of cubic and hexagonal ice crystals with I_{44}/I_{40} value of 0.28±0.01 (triplicate experiments). This suggests that, in this temperature range, water mobility is too low to form hexagonal crystals on the time scale of the experiment. When the sample was heated up to -30 °C, the I_{44}/I_{40} ratio rose to 0.39, indicating a shift from cubic to hexagonal ice. Further temperature increase up to -20 °C resulted in the maximum ratio value (i.e. $I_{44}/I_{40} = 0.82$), meaning that all the ice in the sample has changed into hexagonal form. These results are in agreement with reported[31] XRD patterns of ice crystals in highly concentrated glucose solutions that described the transformation of cubic ice crystals into hexagonal ones during heating.

3.3 Crystal growth in concentrated systems

DSC and cryo-XRD results demonstrate that primary nucleation (i.e. spontaneous crystallisation) becomes increasingly difficult as solids concentration increases, with 26 °C supercooling required for crystallisation to occur spontaneously in a 60% sucrose solution (cooling

rate 1 °C/min), as shown in Figure 3(a) (zoomed scan). Therefore, to study crystal growth at higher - and industrially more relevant - temperatures, an ice seed was added to a supercooled solution and crystal growth was observed under the microscope. Supercooling (ΔT) was defined as the difference between the droplet's temperature prior the addition of the seed crystal[32], controlled by the Linkam stage, and the equilibrium freezing temperature. As the Biot number of the supercooled droplets (before the addition of the seed crystal) was Bi < 0.1, the temperature of the samples was assumed to be that of the stage[34] for supercooling calculation purposes. Equilibrium freezing temperatures for the 40%, 50%, and 60% sucrose solutions were assumed at -4.4 °C, -7.0 °C, and -11.4 °C, respectively. For the 60% system, preliminary results confirmed that supercooling up to 9 °C (temperature of -20 °C) was insufficient to induce nucleation at the experimental time scale - i.e. no crystals were observed after 1 hour, as shown in Figure 5(a),(b) and (c) - while after the addition of an ice seed crystal growth occurred in a time scale of minutes (Figure 5 (d),(e) and (f)), even at supercooling as low as 5 °C, this is T= -16 °C.

3.3.1 Crystal growth in sucrose solutions

The effect of both solute content and supercooling (ΔT) on the growth rate of ice crystals was investigated for solutions with concentrations of sucrose between 40% and 60% w/w. The dependence of the growth rate on ΔT was described by a power law of the form[33]:

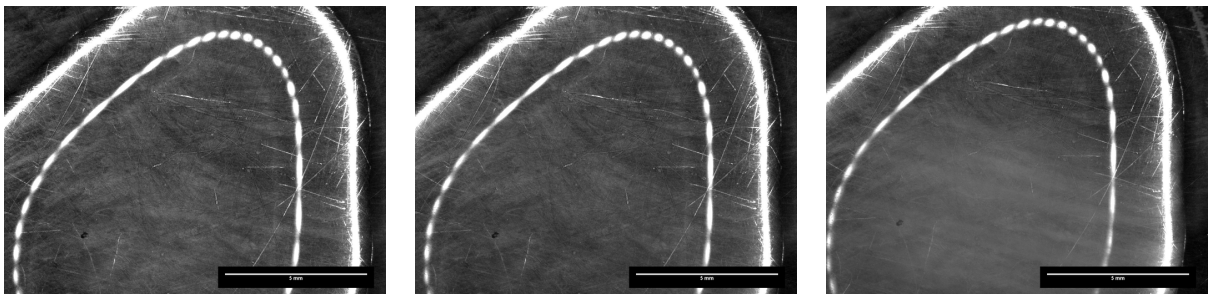

(a) (b) (c)

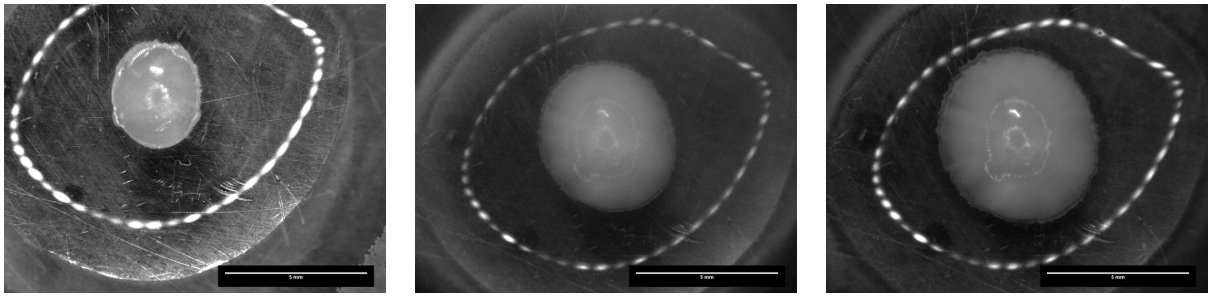

(d) (e) (f)

Figure 5. Microscope images for the system without seed recorded at (a) 0 min (b) 30 min (c) 60 ; Microscope images for the system with seed recorded (d) 0 min (e) 1 min and (f) 2 minutes after adding ice seed into a 60% sucrose droplet at -20 °C. Scale bar=5mm. Bright circles in the images are due to LED light reflection.

$$G = k_G \Delta T^g \quad (7)$$

where G (m s^{-1}) is the crystal growth velocity, k_G is the growth rate constant (m $^oC^{-1}$ s^{-1}) and g is an order parameter.

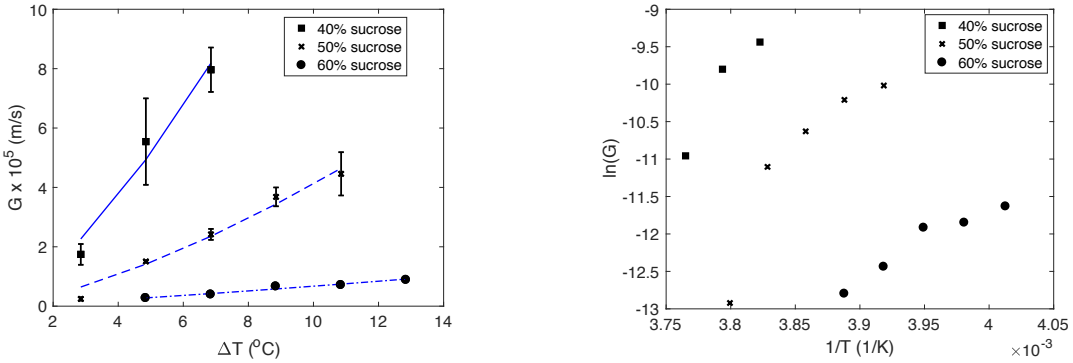

(a) (b)

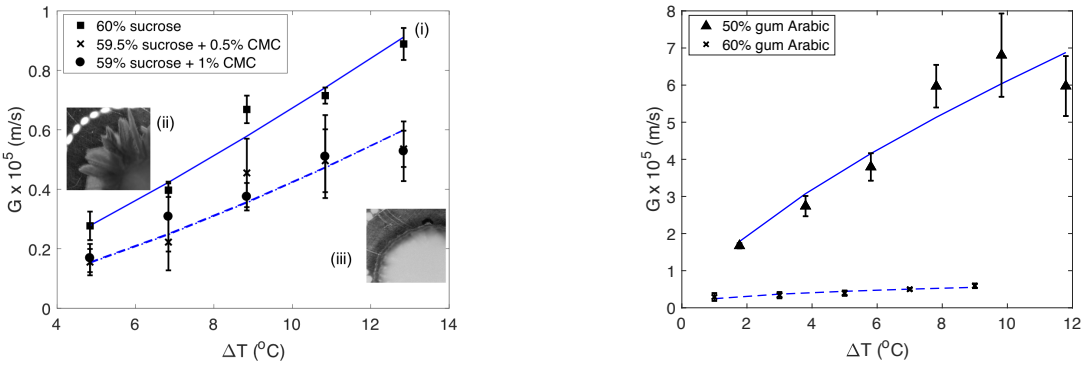

Figure 6. (a) Effect of supercooling and concentration on crystal growth rate (G) in sucrose systems with 40% (squares), 50% (crosses) and 60% (dots) solids; (b) Arrhenius plot of crystal growth from seed: logarithm of crystal growth rate as a function of reciprocal of the temperature; (c) (i) Effect of temperature and viscosity (addition of CMC) on growth rate from sucrose solutions with 40% water content; Zoom-in images of ice crystals developed from 60% sucrose solutions at (ii) 13 °C supercooling (-24 °C) and (iii) 5 °C supercooling (-16 °C). Image width: 4mm. CMC curves are overlapping; (d) Effect of supercooling and concentration on crystal growth of gum arabic systems. In (a), (c) and (d) lines correspond to the power law fit defined in equation (5).

Figure 6(a) presents the variation of measured crystal growth velocities at different ΔT, as well as the fit of Equation (7) for each concentration of sucrose (lines). Results showed higher crystal growth velocities as supercooling increased: up to 4 times higher for the 40% system as ΔT increased from 3 °C to 7 °C, and twice as fast for the 60% sucrose when ΔT increased from 5 °C to 13 °C. In addition, the 40% and 50% sucrose systems showed a faster rise (higher slope) of experimentally measured growth rates for ΔT > 4.5 °C. Although this observation is based on a single point below ΔT= 4.5 °C (albeit for triplicated experiments), it is in accordance with previous

studies on sucrose systems that identified $\Delta T=4.5\ ^{o}C$ as the critical supercooling marking the change from thermally controlled growth to kinetically controlled ice crystal growth in sucrose solutions[34].

Crystal growth rates were slower on increasing solid concentration (see Figure 6(b)). For example, at $\Delta T = 7\ ^{o}C$ the growth rate was reduced by 70% (from $8x10^{-5}$ to $2.4x10^{-5}$ m s^{-1}) as the sucrose concentration increased from 40% to 50%, and by 95% (to $4x10^{-6}$ m s^{-1}) on further increase to 60% sucrose. Similar trends were found for the estimated growth rate constant k_G, which decreased an order of magnitude - from 4.88 $x10^{-6}$ m $^{o}C^{-1}s^{-1}$ to 4.08 $x10^{-7}$ $m^{o}C^{-1}s^{-1}$- as the initial sucrose content increased from 40% to 60% w/w (values listed in Table 1, alongside estimated order parameters *g* for all the investigated systems). The estimated *g* values for the sucrose systems are in the range between 1.2 and 1.5, which is consistent with reported values, typically between 1 and 2.4 [33-37]. Adding solids both slows down heat transfer and reduces molecular mobility[38], which causes a significant decrease of the crystal growth rate: as ice forms from water, sucrose molecules must be displaced from the ice front, and this becomes more difficult with increasing solids concentrations.

Table 1. Growth rate constants (m $^{o}C^{-1}s^{-1}$), order parameter and coefficient of determination obtained from regression analysis within a 95% interval of confidence using Equation (7) for all the system studied.

	k_G	g	R^2
40% sucrose	4.88 x 10^{-6}	1.46	0.97
50% sucrose	1.37 x 10^{-6}	1.47	0.98
60% sucrose	4.07 x 10^{-7}	1.22	0.96

59.5% sucrose + 0.5% CMC	1.75×10^{-7}	1.39	0.88
59% sucrose + 1% CMC	1.67×10^{-7}	1.40	0.89
50% gum Arabic	1.19×10^{-5}	0.71	0.89
60% gum Arabic	2.45×10^{-6}	0.37	0.88

Figure 6(b) presents the Arrhenius plot – i.e. lnG vs. 1/T – for the investigated sucrose systems. Activation energy values were estimated from the slopes of the lines. Data in this graph suggest that for 40% and 50% sucrose solutions two slopes can be fitted in the Arrhenius plots, with ΔT = 4.5 °C as the change point. The smaller slopes observed for $\Delta T > 4.5$ °C indicate a decrease of the activation energy for lower temperatures, compared to that at $\Delta T < 4.5$ °C, as listed in Table 2. This slope reduction indicates a growth rate less dependent on temperature[19], thus suggesting a shift in the controlling mechanism of ice crystal growth in sucrose systems for $\Delta T > 4.5$ °C [34].

For the investigated conditions, all the sucrose systems presented estimated E_a values larger than the theoretical E_a^D (see Table 2), especially those corresponding to higher temperatures and thus slower growth rates (smoother slope in Figure 6(a), E_{a1} in Table 2), which indicates that diffusion is not the main controlling growth mechanism. As temperature decreased, diffusion effects became increasingly significant[21], and E_{a2} values get closer to E_{aD} ones, (see Table 2). In addition, increasing the solid concentration was associated to a slope decrease in the Arrhenius plot, and thus a decrease in the activation energy as well[19]: the 60% solution exhibited lower activation energy values, compared to the 40% and 50% solids systems, revealing a shift towards a more diffusion-controlled growth mechanism.

To calculate the theoretical E_{aD} values used in this analysis, the self-diffusivity of water in sucrose solutions was calculated using Equation (4) and published sucrose-water parameters[22]

Table 2. Activation energy obtained from regression analysis within a 95% interval of confidence using the Arrhenius plot of Equation (3) for all the system studied.

	E_{a1} (kJ/mol) $\Delta T<4.5^{o}C$	E_{a2}(kJ/mol) $\Delta T>4.5^{o}C$	E_a^D(kJ/mol)
40% sucrose	336.64	103.88	46.41
50% sucrose	519.37	101.79	40.27
60% sucrose	-	77.62	37.54
59.5% sucrose + 0.5% CMC	87.19	-	
59% sucrose + 1% CMC	73.96	-	
50% gum Arabic	76.37	-	
60% gum Arabic	48.18	-	

3.3.2 Crystal morphology

Different crystal shapes were observed depending on the growth rate, examples for 60% sucrose (40% water) systems are shown in Figure 6(c). The close-ups of the ice crystals in Figure 6(c) show crystals with smooth and round edges when crystallisation occurred at high supercooling (ΔT of about 10 °C), while at slower crystallisation (ΔT of about 5 °C) dendritic crystal patterns were obtained. The latter are characteristic of diffusion controlled solid/liquid interface dynamics[39]. The effect of supercooling on the morphology of the crystals formed has been also

reported at lower solid concetrations[34]: dendritic crystals in 20% sucrose droplets at $\Delta T = 13.5$ °C, while cellular structures were obtained in the same system at $\Delta T = 18$ °C.

3.3.3 Sucrose-CMC systems

To investigate the effect of viscosity on the ice crystal growth rate, the viscosity of the system was increased by adding CMC while maintaining the water content constant at 40%, as described in Section 2.1. Results presented in Figure 6(c) reveal decreasing growth velocities as the viscosity of the system increased, with an overall 40% reduction of the growth rate on addition of the thickening hydrocolloid. Adding 0.5% or 1% CMC showed marginal differences in determining crystal growth kinetics. The estimated k_G values obtained for the solutions with CMC (see Table 1) followed the same trend: the systems with CMC presented values very similar and approximately 35% lower than those of the solution without CMC. The change in viscosity (addition of CMC) showed little effect on the estimated activation energies, (see Table 2).

3.3.4 Gum arabic

Growth rates at different crystallisation temperatures in 50% and 60% gum arabic systems are shown in Figure 6(d). The equilibrium freezing temperature employed for supercooling calculations was obtained from literature[40] and previous work[41]: -6.2 °C and -15 °C for the 50% and 60% gum arabic solutions, respectively.

For the 50% gum arabic system, crystallisation was observed at supercooling $\Delta T = 2$ °C and crystals grew at a rate of 1.67×10^{-5} m s^{-1}. When supercooling increased from $\Delta T = 2$ °C to $\Delta T = 10$ °C, the growth rate increased monotonically reaching a maximum at $\Delta T = 10$ °C ($G = 6.81 \times 10^{-5}$ m

s^{-1}), while further temperature decrease (see point at ΔT =12 °C) appeared to have little effect on the growth rate, albeit within experimental error. This might indicate a change in the limiting mechanism of crystallisation from thermally-controlled to kinetically-controlled[39] that cannot be properly described using the power law given by equation (7) (R^2 = 0.89, in Table 1).

Increasing solid concentration to 60% slowed down crystal growth significantly to values below $6x10^{-6}$ m s^{-1}. For the 60% gum arabic system, the minimum supercooling required for crystal growth was ΔT =1 °C. With increasing supercooling from ΔT =1 °C to ΔT =9 °C, the growth rate appeared to increase, although maintaining low values (almost an order of magnitude lower) in comparison to the 50% solution. The E_a estimated for the 60% gum arabic system (E_a = 48.17 kJ/mol) was slightly lower than the one for the 50% solution (E_a = 76.37 kJ/mol), but closer to the theoretical diffusion-controlled values calculated for sucrose solutions (see Table 2).

3.3.5 Comparison between sucrose & gum arabic systems

Direct, quantitative comparison of ice crystallisation in sucrose solutions and gum arabic is limited due to the different nature of the material: sucrose is a disaccharide of glucose and fructose, whereas gum arabic is a complex mixture of polysaccharides and glycoproteins. However, a qualitative comparison may be relevant to this work, as it can help to understand the role of molecular weight in similarly concentrated carbohydrate systems.

Compared with the case of sucrose solutions, water crystallisation in gum arabic was faster (by $1.5x10^{-5}$ m s^{-1}) at 50% solids and slower (by about $3x10^{-5}$ m s^{-1}) at 60% concentration for similar supercooling. Sucrose has been reported to be more effective in terms of slowing down water crystallisation than many hydrocolloids[38] and this may be the case of 50% solids. However, on increasing concentration to 60% it appears that the high molecular weight hydrocolloid induces

faster water crystallisation rates. This might result from the high viscosity of the highly concentrated gum arabic system, and also from the existence of air bubbles in the sample (at this concentration it was impossible to free the system completely of all air bubbles). Molecular mobility is limited in high viscous systems and thus crystal growth is retarded. Air bubbles may delay water crystallisation in two ways: (i) by slowing down the rate of heat transfer due to poor thermal conductivity[42] and (ii) physically, by taking the space in solution which might slow down mass transfer[43].

4 Conclusions

This work demonstrates the potential to control ice crystal formation during cooling at a range of concentrations, specifically for highly concentrated systems (up to 60% solids) by understanding the link between ice crystallisation and both formulation (e.g. viscosity of the system, solids content) and freezing conditions (e.g. supercooling; nucleation). Primary crystallisation was studied using DSC and XRD, while crystal growth was studied with a novel optical device that allows microscopic visualisation of the system under well controlled supercooled conditions. Results presented highlight the difficulties associated with spontaneous (primary) crystallisation in highly concentrated systems and reveal the potential of promoting and controlling crystal growth by addition of a crystal seed in such challenging systems. The findings of this work have also revealed the influence of formulation (e.g. solid content, water mobility) and crystallisation conditions (e.g. supercooling) on crystal morphology, which has a direct impact on the design of novel processes targeting relevant (bio)product microstructures.

Overall, this work represents a significant contribution to the understanding of water crystallisation dynamics in concentrated systems, which is critical to expand the range of operation

of current freezing and/or freeze-drying operations. In particular, these findings can also help to the design of optimal and more sustainable manufacture methods, as processing highly concentrated systems can help to reduce both energy demand and water usage during crystallisation processes.

ACKNOWLEDGMENTS

The authors would like to thank financial support received from InnovateUK (grant no. TS/K003909/1) and EPSRC (grant no. EP/K011820/1).

REFERENCES

1. Aguilera, J.M. Why food microstructure? *J. Food Eng.* **2005**, *67*, 3-11. DOI: 10.1016/j.jfoodeng.2004.05.050.

2. Joardder, M.U.H.; Kumar, C.; Karim, M.A. Food structure: Its formation and relationships with other properties. *Crit. Rev. Food Sci. Nutr.* **2017**, *57*, 1190-1205. DOI: 10.1080/10408398.2014.971354.

3. Sanz, P.D.; De Elvira, C.; Martino, M.; Zaritzky, N.; Otero, L.; Carrasco, J.A. Freezing rate simulation as an aid to reducing crystallization damage in foods. *Meat Sci.* **1999**, *52*, 275-278. DOI: 10.1016/S0309-1740(99)00002-9.

4. Sigurgisladottir, S.; Ingvarsdottir, H.; Torrissen, O. J.; Cardinal, M.; Hafsteinsson, H. Effects of freezing/thawing on the microstructure and the texture of smoked Atlantic salmon (Salmo salar). *Food Res. Int.* **2000**, *33*, 857-865. DOI: 10.1016/S0963-9969(00)00105-8.

5. Hartel, R.W. Ice crystallization during the manufacture of ice cream. *Trends Food Sci. Technol.* **1996**, *7*, 315-321. DOI: 10.1016/0924-2244(96)10033-9.

6. Petzold, G.; Aguilera, J.M. Ice morphology: fundamentals and technological applications in foods. *Food Biophys.* **2009**, *4*, 378:396. DOI: 10.1007/s11483-009-9136-5.

7. Ishwarya, S.P.; Anandharamakrishnan, C. Spray-Freeze-Drying approach for soluble coffee processing and its effect on quality characteristics. *J. Food Eng.* **2015**, *149*, 171-180. DOI: 10.1016/j.jfoodeng.2014.10.011.

8. Fissore, D.; Pisano, R.; Barresi, A. A. Applying quality-by-design to develop a coffee freeze-drying process. *J. Food Eng.* **2014**, *123*, 179-187. DOI: 10.1016/j.jfoodeng.2013.09.018.

9. Hartel, R.W.; Chung, M.S. Contact nucleation of ice in fluid dairy products. *J. Food Eng.* **1993**, *18*, 281-296. DOI: 10.1016/0260-8774(93)90091-W.

10. Hartel, R.W.; Ergun, R.; Vogel, S. Phase/state transitions of confectionery sweeteners: thermodynamic and kinetic aspects. *Compr. Rev. Food Sci. Food Saf.* **2011**, *10*, 17-32. DOI: 10.1111/j.1541-4337.2010.00136.x.

11. Goff, H.D.; Sahagian, M.E. Glass transitions in aqueous carbohydrate solutions and their relevance to frozen food stability. *Thermochim. Acta* **1996**, *280/281*, 449-464. DOI: 10.1016/0040-6031(95)02656-8.

12. Luyet, B. The problem of structural instability and molecular mobility in aqueous solutions "solidified" at low temperatures (present status and future prospects). *Biodynamica* **1966**, *10*, 1-32.

13. Roos, Y.H.; Taylor, S. *Phase Transitions in Foods*. Elsevier Science, London, **1995**.

14. Omran, A.M.; King, C.J. Kinetics of ice crystallization in sugar solutions and fruit juices. *AIChE J*. **1974**, *20*, 795-803. DOI: 10.1002/aic.690200422.

15. Shirai, Y.; Wakisaka, M.; Miyawaki, O.; Sakashita, S. Effect of seed ice on formation of tube ice with high purity for a freeze wastewater treatment system with a bubble-flow circulator. *Water Research* **1999**, *33*, 1325-1329. DOI: 10.1016/S0043-1354(98)00335-2.

16. Garside, J.; Mersmann, A.; Nývlt, J. *Measurement of crystal growth and nucleation rates*. IChemE, Rugby, UK, **2002**.

17. Levine, H.; Slade, L. A polymer physico-chemical approach to the study of commercial starch hydrolysis products (SHPs). *Carbohydr. Polym.* **1986**, *6*, 213-244. DOI: 10.1016/0144-8617(86)90021-4.

18. Roos, Y.; Karel, M. Amorphous state and delayed ice formation in sucrose solutions. *Int. J. Food Sci. Technol.* **1991**, *26*, 553-566. DOI: 10.1111/j.1365-2621.1991.tb02001.x

19. Atkins, P.; de Paula, J.; Friedman, R. *Physical Chemistry: Quanta, Matter, and Change*. OUP Oxford, **2013**.

20. McNaught, A.D. *Compendium of chemical terminology*. Blackwell Science Oxford, **1997**.

21. Mullin, J.W. *Crystallization*. 4th Edition. Elsevier Science, Oxford, **2001**.

22. Van Der Sman, R.G.M.; Meinders, M.B.J. Moisture diffusivity in food materials. *Food Chem.* **2013**, *138*, 1265-1274. DOI: 10.1016/j.foodchem.2012.10.062.

23. Roos, Y.; Karel, M. Phase transitions of amorphous sucrose and frozen sucrose solutions. *J. Food Sci.* **1991**, *56*, 266-267. DOI: 10.1111/j.1365-2621.1991.tb08029.x.

24. Schawe, J.E.K. A quantitative DSC analysis of the metastable phase behavior of the sucrose–water system. *Thermochim. Acta* **2006**, *451*, 115-125. DOI: 10.1016/j.tca.2006.09.015.

25. Furuki, T. Effect of molecular structure on thermodynamic properties of carbohydrates. A calorimetric study of aqueous di- and oligosaccharides at subzero temperatures. *Carbohydr. Res.* **2002**, *337*, 441-450. DOI: 10.1016/S0008-6215(01)00332-9.

26. Dowell, L.G.; Moline, S.W.; Rinfret, A.P. A low-temperature X-ray diffraction study of ice structures formed in aqueous gelatin gels. *Biochim. Biophys. Acta* **1962**, *59*, 158-167. DOI: 10.1016/0006-3002(62)90706-0.

27. Dowell, L.G.; Rinfret, A.P. Low-temperature forms of ice as studied by X-ray diffraction. *Nature* **1960**, *188*, 1144-1148. DOI: 10.1038/1881144a0.

28. Murphy, D. Dehydration in cold clouds is enhanced by a transition from cubic to hexagonal ice. *Geophys. Res. Lett.* **2003**, *30*, 2230. DOI: 10.1029/2003GL018566.

29. Fletcher, N.H. *The Chemical Physics of Ice*. Cambridge University Press, **1970**.

30. Murray, B.J.; Knopf, D.A.; Bertram, A.K. The formation of cubic ice under conditions relevant to Earth's atmosphere. *Nature* **2005**, *434*, 202-205. DOI: 10.1038/nature03403.

31. Thanatuksorn, P.; Kajiwara, K.; Murase, N.; Franks, F. Freeze–thaw behaviour of aqueous glucose solutions—the crystallisation of cubic ice. *Phys. Chem. Chem. Phys.* **2008**, *10*, 5452. DOI: 10.1039/b802042f.

32. Young, F.E.; Jones, F.T. Sucrose hydrates. The sucrose-water phase diagram. *J. Phys. Chem.* **1949**, *53*, 1334-1350. DOI: 10.1021/j150474a004.

33. Teraoka, Y.; Saito, A.; Okawa, S. Ice crystal growth in supercooled solution. *Int. J. Refrig.* **2002**, *25*, 218-225. DOI: 10.1016/S0140-7007(01)00082-2.

34. Hindmarsh, J.P.; Russell, A.B.; Chen, X.D. Measuring dendritic growth in undercooled sucrose solution droplets. *J. Cryst. Growth* **2005**, *285*, 236-248. DOI: 10.1016/j.jcrysgro.2005.08.017.

35. Hallett, J. Experimental studies of the crystallization of supercooled water. *J. Atmos. Sci.* **1964**, *21*, 671-682. DOI: 10.1175/1520-0469(1964)021<0671:ESOTCO>2.0.CO;2.

36. Kallungal, J.P.; Barduhn, A.J. Growth rate of an ice crystal in subcooled pure water. *AIChE J.* **1977**, *23*, 294-303. DOI: 10.1002/aic.690230312.

37. Ayel, V.; Lottin, O.; Faucheux, M.; Sallier, D.; Peerhossaini, H. Crystallisation of undercooled aqueous solutions: Experimental study of free dendritic growth in cylindrical geometry. *Int. J. Heat Mass Transfer* **2006**, *49*, 1876-1884. DOI: 10.1016/j.ijheatmasstransfer.2005.10.036.

38. Budiaman, E.R.; Fennema, O. Linear rate of water crystallization as influenced by temperature of hydrocolloid suspensions. *J. Dairy Sci.* **1987**, *70*, 534-546. DOI: 10.3168/jds.S0022-0302(87)80038-3.

39. Shibkov, A.A.; Zheltov, M.A.; Korolev, A.A.; Kazakov, A.A.; Leonov, A.A. Crossover from diffusion-limited to kinetics-limited growth of ice crystals. *J. Cryst. Growth* **2005**, *285*, 215-227. DOI: 10.1016/j.jcrysgro.2005.08.007.

40. Mothé, C.G.; Rao, M.A. Thermal behavior of gum arabic in comparison with cashew gum. *Thermochim. Acta* **2000**, *357/358*, 9-13. DOI: 10.1016/S0040-6031(00)00358-0.

41. Malik, N.; Gouseti, O.; Bakalis, S. Effect of freezing on microstructure and reconstitution of freeze-dried high solid hydrocolloid-based systems. *Food Hydrocolloids* **2018**, *83*, 473-484. DOI: 10.1016/j.foodhyd.2018.05.008.

42. Sofjan, R.P.; Hartel, R.W. Effects of overrun on structural and physical characteristics of ice cream. *Int. Dairy J.* **2004**, *14*, 255-262. DOI: 10.1016/j.idairyj.2003.08.005.

43. Cook, K.L.K.; Hartel, R.W. Mechanisms of ice crystallization in ice cream production. *Compr. Reviews Food Sci. Food Saf.* **2010**, *9*, 213-222. DOI: 10.1111/j.1541-4337.2009.00101.x.

Author Contributions

The manuscript was written through contributions of all authors. All authors have given approval to the final version of the manuscript.

Funding Sources

InnovateUK (grant no. TS/K003909/1) and EPSRC (grant no. EP/K011820/1).